



Published in final edited form as:

Alcohol Clin Exp Res. 2010 April ; 34(4): 669–680. doi:10.1111/j.1530-0277.2009.01136.x.

Event-related oscillations vs. event-related potentials in a P300 task as biomarkers for alcoholism

Colin Andrew, Ph.D^{1,2,3} and George Fein, Ph.D^{1,4,*}

¹Neurobehavioral Research Inc

²Department of Human Biology, Faculty of Health Sciences, University of Cape Town

³Department of Psychiatry, Faculty of Health Sciences, University of Stellenbosch

⁴Department of Psychology, University of Hawaii

Abstract

OBJECTIVE—It has been proposed that event-related oscillation (ERO) measures of EEG activity recorded in P300 tasks provide more powerful biomarkers of alcoholism than event-related potential (ERP) measures. This study examines this question in a group of long-term abstinent alcoholics (LTAAAs).

METHODS—EEGs were recorded on 48 LTAAAs and 48 age and gender matched non-alcoholic controls (NACs) during the performance of a 3-condition visual target detection task. The event-related data were analyzed to extract ERP amplitude measures and total and evoked ERO power measures. Data were analyzed using MANCOVA to determine the contributions of ERO vs. ERP measures to discriminate between the LTAA vs. NAC groups.

RESULTS—The LTAA group showed significantly lower evoked δ ERO power and total δ and θ ERO power compared to the control group. The evoked and total ERO power measures provide an alternative (but not more powerful) representation of the group difference than does P3b amplitude. There was a weak suggestion that non-phase-locked θ ERO power (which contributes to total ERO power) might provide independent discriminatory information.

CONCLUSIONS—Reduced evoked ERO power in the response to target stimuli provided an alternative and comparable representation of the reduced P3b amplitude in LTAA. This is not surprising since the evoked ERO power measures are derived from time-frequency representations (TFRs) of the ERP waveform. Induced theta oscillations might provide independent discriminatory information beyond ERP amplitude measures, but separate analysis of the event-related non-phase-locked activity is required to investigate this further.

Keywords

EEG; Event-related potentials; Event-related oscillations; Alcoholism; P300; P3b; Biomarker

INTRODUCTION

A large body of evidence suggests that alcoholics process stimuli differently from non-alcoholics, and that electrophysiological measures of stimulus processing discriminate groups of alcoholics from non-alcoholics and groups of individuals at high risk of developing alcoholism from groups not at high risk. One of the most robust findings in

*Address reprints and correspondence to: George Fein, Ph.D, Neurobehavioral Research Inc. 1585 Kapiolani Blvd. Ste. 1030, Honolulu, HI 96814, USA, Phone:(808) 237-5407, Fax:(808) 442-1156, george@nbresearch.com.

electrophysiological alcoholism research is the reduction in the amplitude of the P3b ERP component in alcoholics and in high risk individuals (1984; Begleiter et al., 1987; Benegal et al., 1995; Berman et al., 1993; Cohen et al., 1997; Ehlers et al., 2003; Fein and Chang, 2006; Glenn et al., 1994; Glenn et al., 1996; Hill and Steinhauer, 1993; Iacono et al., 2003; Kamarajan et al., 2005; O'Connor et al., 1986; O'Connor et al., 1987; Polich et al., 1994; Porjesz and Begleiter, 1985; 1990; Porjesz et al., 1998; Steinhauer and Hill, 1993; Suresh et al., 2003; Van der Stelt et al., 1998). The P3b is a subcategory of the P300, and occurs when an individual attends or responds to an infrequent but task-relevant target stimulus. It is defined as a centro-parietal positive voltage peak in the ERP waveform occurring between 300 to 500 milliseconds after stimulus presentation.

In addition to eliciting an ERP, an endogenous or exogenous event can also result in frequency-specific changes to ongoing EEG oscillations that are not phase locked to the stimulus and so cannot be extracted by trial averaging. (Pfurtscheller and Lopes da Silva, 1999). Spectral analysis techniques, such as time-frequency analysis, are applied to the event-related trials to quantify such changes. In such event-related oscillation (ERO) analyses, the dynamics of the power of frequency-specific oscillations are quantified and these spatiotemporal dynamics are examined as they relate to task-specific sensory, motor and/or cognitive processes. Event-related decreases (increases) of power in specific frequency bands are considered to be due to decreases (increases) in synchrony of the underlying neuronal assemblies. These synchrony changes are thought to result from event-related changes in the oscillatory control parameters of these neuronal networks. Thus, a relative decrease in band power is often referred to as event-related desynchronization (ERD) and a relative power increase as an event-related synchronization (ERS). An event-related increase in non-phase-locked frequency-specific activity is also often referred to as an induced oscillation (Pfurtscheller and Lopes da Silva, 1999).

Spectral analysis can also be applied directly to the ERP waveforms to quantify the underlying oscillatory nature of these waveforms. The spectral decomposition of the phase-locked activity may reveal evoked oscillations, often in the theta and alpha bands. The study of evoked oscillations has led to the proposition of an oscillatory model in comparison to the classic evoked model of the ERP. While the evoked model ascribes ERP generation to the superposition of a series of transient post-synaptic responses of pyramidal neurons that are independent of ongoing EEG oscillations (Pfurtscheller and Lopes da Silva, 1999), the oscillatory model accounts for the ERP through (i) partial phase resetting of the ongoing oscillations, with amplitude enhancement occurring through trial averaging of the phase-locked oscillations or (ii) phase-dependent amplitude modulation within single trials (Basar-Eroglu et al., 1992; Fell et al., 2004; Gruber et al., 2005; Klimesch, 1999; Klimesch et al., 2004; Kolev et al., 1997; Makeig et al., 2002; Penny et al., 2002; Schurmann et al., 2001; Shah et al., 2004; Yordanova et al., 2003). Limitations in methodology often make it difficult to disentangle phase resetting from additive evoked responses (Sauseng et al., 2007), and so it is therefore difficult to draw definitive conclusions regarding which of these mechanisms underlies the generation of the ERP¹.

In the search for biomarkers of alcoholism, ERO measures that index brain functions associated with stimulus processing are an attractive proposition, as they may provide complementary information to that of the ERP measures. For this reason, a number of studies on alcoholism have investigated ERO measures extracted from EEG data collected during the performance of stimulus processing tasks (Jones et al., 2006; Kamarajan et al.,

¹Evidence for the oscillatory hypothesis of ERP genesis needs to be presented, for example by demonstrating an underlying phase reset mechanism of ongoing oscillations, in order to infer a correspondence between the oscillatory basis functions of the time-frequency representation and neurophysiological oscillations.

2006; Kamarajan et al., 2004; Porjesz and Begleiter, 2003; Rangaswamy et al., 2007). Jones et al. (2006) conducted ERO analysis to compare adult male alcoholics and controls on a 3-condition visual target detection task. The same research group (Rangaswamy et al., 2007) applied this methodology to compare high risk vs. low-risk groups of adolescents, seeking trait (or endophenotypic) markers of the vulnerability to develop alcoholism.

In both studies (Jones et al., 2006; Rangaswamy et al., 2007), ERP amplitude measures and ERO measures in different sub-bands across delta, theta and alpha frequency bands were extracted from the event-related data. Two types of ERO measures were quantified: (i) evoked ERO power measures were computed by applying time-frequency analysis directly to the trial-averaged ERP waveforms and (ii) total ERO power measures were calculated by applying time-frequency analysis to each individual trial and averaging the results across trials. Total ERO power contains contributions from both phase-locked and non-phase-locked activity, while evoked ERO power quantifies phase-locked activity only. Multivariate analysis of variance (MANOVA) was applied to the ERP and ERO measures to investigate which measures best discriminated the groups. The principle finding was that in addition to the P3b amplitude, the δ evoked power and the θ total power significantly distinguished the two groups from one another. Both studies concluded that the ERO power measures provided unique information beyond that of the ERP measures for group discrimination. While there was agreement between the two studies that ERO measures discriminated the groups, Jones et al. (2006) found that δ evoked power and θ total power over frontal regions provided the best discrimination, while Rangaswamy et al. (2007) found that δ evoked power over parietal regions and θ total power at central and parietal sites best discriminated the groups.

As the ERO power measures quantify the ERP waveform dynamics within a time window, it is possible that they contain additional group discriminatory information to the ERP amplitude measure, when this measure is only quantified at a single time point in the ERP waveform². As the total ERO power measures contain contributions from both phase-locked and non-phase-locked oscillations, the contributions of non-phase-locked induced oscillations might provide independent information to that of the ERP amplitude measure. This could account for the finding reported in the Jones et al. (2006) and Rangaswamy et al. (2007) studies that the ERO measures provided group discriminators that were more powerful than the ERP amplitude measures.

However, to provide strong evidence for such a conclusion, either a statistical comparison of group effect sizes of the ERO and ERP measures is required or an analysis of covariance should be undertaken to assess whether the variance of the ERO power measures remaining, after the covariance between the ERP and ERO measures is removed, significantly discriminates the two groups. Such methods were not applied in the Jones et al. (2006) and Rangaswamy et al. (2007) studies (group effect sizes were not even presented), and so the conclusions made were not supported by quantitative analysis.

The objective of the current study was to compare ERO vs. ERP measures in discriminating long-term abstinent alcoholics (LTAA) from age and gender comparable non-alcoholic controls (NACs) in a visual 3 condition target detection task. Appropriate statistical analyses were applied to determine whether the ERO power measures provided more powerful discrimination between groups.

²Transforming the ERP waveform into the time-frequency domain does not produce new information, but simply creates an alternative representation of the information present in the time domain waveform. Therefore, differences found in the discriminatory power of the evoked ERO and ERP measures in the Jones et al. (2006) and Rangaswamy et al. (2007) studies would only be the result of using a considerably larger temporal extent of the waveform than using point (ERP amplitude) measures.

MATERIALS AND METHODS

Subjects

Various advertising methods (newspaper advertisements, Internet postings etc.) were used to recruit the study participants. The study comprised of LTAAAs and age and gender matched NACs. Each group consisted of 23 females and 25 males aged 35 to 58 (mean = 46.3, SD = 6.8). Inclusion criteria for the LTAA group were meeting DSM-IV (American Psychiatric Association, 2000) criteria for alcohol dependence and being abstinent for at least six months. NAC participants responded to advertisements for light/non-drinkers and were recruited if they did not meet lifetime criteria for alcohol abuse or dependence, had a lifetime drinking average of less than 30 drinks/mo and never drank more than 60 drinks/mo. For a more detailed account of the subject selection methodology and the neuropsychological and clinical assessments administered, the reader is referred to Fein & Chang (2006).

VP3 Experimental Paradigm

The visual oddball experiment was administered using the E-prime software system (Psychology Software Tools Inc., Pittsburgh, USA). The task consisted of the presentation of three types of visual stimuli:- (i) standard non-target stimuli – a small hollow white square; (ii) target stimuli – a small white X; and (iii) rare non-target stimuli – different shapes of various colors. The stimuli were displayed for 200ms in the middle of a black screen on a computer monitor, followed by a delay varying between 1000ms and 1100ms before the next stimulus and during which time the screen was blank. Stimuli were presented in a predetermined semi-random order, with standard non-target stimuli appearing 210 times, rare non-target stimuli appearing 35 times and target stimuli appearing 35 times. The total task duration was approximately 6.5 minutes. The subjects were instructed not to respond to the standard and rare non-target stimuli, and to press a response key as quickly as possible to target stimuli. Each subject was shown examples of the various stimuli during a short practice session before proceeding with the task. The paradigm was similar to that used by Jones et al. (2006) and Rangaswamy et al. (2007), with differences being that those studies presented stimuli for only 60 ms and had longer and fixed ISIs of 1600 ms (Jones et al., 2006) and 1625 ms (Rangaswamy et al., 2007).

EEG Acquisition

EEG was acquired on three EEG acquisition systems (with two different amplifiers) during the course of the study. The first two were a 32-channel system (N = 7 subjects) and a 40-channel system (N = 81 subjects), both which used the NuAmps single-ended, 32/40-channel amplifier and Scan 4.2 Acquisition software (Compumedics Neuroscan Inc., El Paso, USA). The third was a 64-channel system (N = 8 subjects) which used the SynAmps2 amplifier and Scan 4.3 acquisition software (Compumedics Neuroscan Inc., El Paso, USA). Electrode sites Fz, FCz, Cz, CPz and Pz, which were the main electrode sites analyzed in this study, were common to all three systems. A right ear reference electrode was used for all recordings. The ground electrode was placed 4 cm above the nasion for the 32-channel and 40-channel caps, and 8 cm above the nasion for the 64-channel caps. Electrode site impedances were kept below 10 k Ω for all recordings. A vertical electro-oculogram (EOG) was recorded from a bipolar electrode site pair placed above and below the left eye for use in offline reduction of ocular artifacts. The EEG and EOG channels were sampled at 250 Hz and stored for offline analysis.

To ensure that between-amplifier comparisons were valid, data from control participants recorded on both amplifier systems (NuAmps, SynAmps2) were examined and revealed no differences associated with the different acquisition amplifiers. Additionally, a within-

amplifier analysis, using only the participants whose data were collected using the NuAmps amplifier, replicated ERP results reported in Fein and Chang (2006) that were produced from the combined data acquired with both amplifiers.

EEG Analysis

The Brain Vision Analyzer package (BVA, Brain Products, Munich, Germany), was utilized for pre-processing of the data, computation of ERP waveforms and extraction of the peak amplitudes of the ERP components. The open-source, MATLAB-based EEGLAB Toolbox (Delorme and Makeig, 2004) was used for computation of event-related TFRs and extraction of ERO power measures from these TFRs, with additional functionality added to the toolbox as required. The methodology used for the analysis of the event-related EEG data, as described below, was similar to the methodology used in Jones et al. (2006) and Rangaswamy et al. (2007), with important differences indicated..

Artifacts were removed using the Gratton and Coles method implemented in BVA (Gratton et al., 1983). Data were then bandpass filtered between 0.5 Hz and 30Hz³ using a zero phase lag filter with a 48 dB/octave roll-off. Stimulus-locked trials were extracted for all instances where there was a correct behavioral response, for each of the three experimental conditions (target, rare non-target and standard non-target), with each trial comprising 450ms of data pre-stimulus and 1300ms post-stimulus⁴. The response window for correct responses on target trials was 800 ms. Data for the ERP analysis were baseline corrected using the 100ms pre-stimulus interval⁵. Any trials containing out of range voltages ($\pm 75 \mu\text{V}$) were rejected as artifacts and excluded from further processing. All further processing was applied to the data from the target condition only.

ERP waveforms were extracted by synchronously averaging all trials having the correct behavioral responses for the target condition, producing one ERP waveform per electrode site per subject. For each subject, the peaks of the major ERP components, these being the N100, P200, N200, P300 (i.e. P3b) and N300, were extracted independently for each of the midline electrode sites of interest (MESOIs)⁶, these being Fz, FCz, Cz, CPz and Pz, using a semi-automated peak detection algorithm. Peak locations were adjusted manually where necessary, and if no discernable peak was present or the locations were ambiguous, the ERP component for that subject was omitted from further analysis. Grand average ERP waveforms and topographical maps for each of the ERP components were computed across groups.

Event-related TFRs were computed using the Stockwell Transform (ST) in two different ways:- (i) the ST transform was applied to each single-trial, resulting in a complex-valued TFR for each trial. The absolute power for each single-trial TFR was then computed by taking the square of the magnitude of the complex-valued TFR for each trial and these were then averaged across all trials to produce a resultant TFR that was termed the event-related total power TFR or ERO_{TOT} TFR. (ii) the ST transform was applied to the trial-averaged ERP waveform, with the absolute power computed by taking the square of the magnitude of the complex-valued TFR, this termed the event-related evoked power TFR or ERO_{EVK} TFR. Using these methods, one ERO_{EVK} TFR and one ERO_{TOT} TFR were produced per electrode

³Jones et al. (2006) and Rangaswamy et al. (2007) used a filter setting of 0.02–100 Hz

⁴The reason that the trial length of 1750 ms was chosen to be slightly longer than the inter-trial interval (ISI) of between 1200ms to 1300ms, was to allow the dynamics of the ERO's to be observed in the TFRs beyond the ISI to ensure that event-related changes of oscillatory activity had returned to baseline levels before the presentation of the next stimulus.

⁵Jones et al. (2006) and Rangaswamy et al. (2007) used a 200ms pre-stimulus interval for baseline correction

⁶Full electrode montage recordings allowed the spatial distributions of ERPs and EROs across the entire scalp surface to be computed. Only midline electrodes were utilized for statistical analysis, as the ERP and ERO spatial topographies showed bilaterally symmetrical distributions centered on the midline (see Results).

site per subject. Based on visual inspection of the distribution of power within the ERO_{EVK} and ERO_{TOT} TFRs at the MESOI, time-frequency regions of interest (TFROIs) were defined, with the sub-bands of these TFROIs covering the δ , θ and α frequency bands and the time windows covering time epochs that overlapped with the major components in the ERP waveforms. The power within each TFROI, for both total and evoked power TFRs, was computed and these ERO_{TOT} and ERO_{EVK} power measures were utilized for further statistical analysis. Grand average ERO_{EVK} TFRs and topographical maps for each of the ERO_{EVK} power measures (δ_1 , δ_2 , θ_1 , θ_2 and α) were computed across subjects.

Statistical Analysis

All statistical analyses were performed using SPSS (SPSS Inc., Chicago, USA). To investigate which of the measures (ERP amplitude measures, evoked ERO power measures or total ERO power measures) discriminated the two groups, MANOVAs were applied. The Pillai-Bartlett trace was used as the test statistic for the MANOVAs. Tests of multivariate normality were not carried out on the dependent variables, but the Kolmogorov-Smirnov test was performed on each dependent variable to check for univariate normality. Where dependent variables were not normally distributed, logarithmic transformation of the variables was applied.

Separate MANOVAs were carried out for each of the ERP amplitude measures (N100, P200, N200, P3b and N300), ERO_{EVK} power measures (δ_1 , δ_2 , θ_1 , θ_2 and α) and ERO_{TOT} power measures (δ_1 , δ_2 , θ_1 , θ_2 and α). For each MANOVA, the particular measure (for example the P3b amplitude measures or the α ERO_{EVK} power measures) at each of the MESOIs were taken as the multiple dependent variables, with group (NAC vs. LTAA) as the between-subjects independent variable. A further MANOVA and a multivariate analysis of covariance (MANCOVA) were performed on a subset of the ERO power measures at selected MESOIs. The measures selected were the ones found to be the best⁷ discriminators of the groups. The covariate utilized for the MANCOVA was an ERP amplitude measure at a selected MESOI found to best⁸ discriminate the groups.

For the MANOVAs (MANCOVA), follow-up analyses were performed to investigate the reasons for significant group effects. Univariate ANOVAs (ANCOVAs) were utilized with each of the dependent variables taken independently. For the MANOVAs, discriminant analysis was also used with the dependent variables taken as the predictors in the discriminant function. Bonferroni corrections for multiple comparisons were not applied to any of the analyses.

RESULTS

(i) ERP Results

(a) ERP waveforms and topographical distributions—Figure 1(a) shows the grand average ERP waveform for the target condition for the NACs at electrode site Cz, together with the topographical distributions of the ERP amplitudes of the major components of the ERP waveform.

(b) Group comparison of ERP amplitudes—Table 1 shows the results of MANOVA analyses applied to the ERP amplitudes measures. The results show that only P200 ($F(5,79) = .139$, $p = .035$) and P3b ($F(5,90) = .195$, $p = .001$) amplitudes discriminate the groups.

⁷Best is defined in terms of the size of the univariate group effect. For each ERO_{EVK} or ERO_{TOT} power measure that showed a significant multivariate group effect, a single ERO power measure at the electrode site which showed the largest univariate group effect across all MESOIs was selected.

⁸Definition as for the best ERO power measure discriminators

However, Box's test on the P200 amplitude measures indicated that the covariance matrices differed significantly between groups ($p = 0.003$), complicating the group comparison on this difference. LTAAAs had reduced P3b amplitudes at Pz and CPz, with the group effect accounting for 8.5% and 4.8% of the variance, respectively. The discriminant analysis support the separate contributions of P3b at Pz and CPz in discriminating the groups

(ii) ERO Results

(a) ERO TFRs and topographical distributions—Figure 1(b) shows the grand average log-transformed ERO_{EVK} TFR at electrode site Cz for the NACs. The power in the ERP is localized to the first 700 ms post stimulus, with peak power occurring from 200 to 500 ms and between 4 to 5 Hz. The ERO_{TOT} TFR at electrode site Cz showed a similar distribution in the delta and theta band, but with the peak value of the theta power being approximately 3 times larger (on a linear scale) in the ERO_{TOT} TFR compared to the ERO_{EVK} TFR. The main difference between TFRs was in the alpha band, where the ERO_{TOT} TFR showed significantly larger pre-stimulus alpha power than in the ERO_{EVK} TFR. The alpha power showed desynchronization (i.e. showed a decrease in power), after stimulus onset, at approximately 200ms post-stimulus, with maximum desynchronization at around 600ms post-stimulus. The alpha power returned to pre-stimulus baseline levels by approximately 1000ms post-stimulus.

Based on visual inspection of the TFRs at the MESOIs, five TFROIs (δ_1 , δ_2 , θ_1 , θ_2 and α), as defined in Table 2 and shown in Figure 1b. were selected for ERO_{EVK} computation. Topographical maps of which shown in Figure 1b. δ_1 and δ_2 ERO_{EVK} power have a midline-symmetrical, parietal localization, with δ_2 ERO_{EVK} power having a more widespread distribution with a slightly more anterior (centro-parietal) peak. The θ_1 and θ_2 ERO_{EVK} power is more anterior than the δ ERO_{EVK} power, with a fronto-central peak. θ_2 ERO_{EVK} power also shows a bilateral peak over the left and right parieto-occipital regions. α ERO_{EVK} power has a bilateral distribution over left and right occipital regions.

(b) Group comparisons of ERO_{EVK} power measures—MANOVAs on each of the ERO_{EVK} log-transformed power measures are shown in Table 3. Only δ_1 ERO_{EVK} power ($F(5,90) = 3.098$, $p = .013$) discriminated the groups. LTAAAs had lower δ_1 ERO_{EVK} power than NACs at Pz, CPz and Cz, with group accounting for 9.9%, 6.3% and 4.8% of the variance respectively. Discriminant analysis confirmed the contribution δ_1 ERO_{EVK} power at Pz, but indicated only δ_1 ERO_{EVK} power at Pz and FCz made independent contributions to group discrimination.

(c) Group comparisons of ERO_{TOT} power measures—MANOVAs on ERO_{TOT} power utilizing log-transformed power at the same TFROIs (δ_1 , δ_2 , θ_1 , θ_2 and α) are shown in Table 4. δ_1 ERO_{TOT} power ($F(5,90) = 3.452$, $p = .007$), θ_1 ERO_{TOT} power ($F(5,90) = 2.567$, $p = .032$) and θ_2 ERO_{TOT} power ($F(5,90) = 2.461$, $p = .039$) discriminated the groups.

Follow-up analyses revealed reduced ERO_{TOT} power in LTAAAs vs. NACs for the:- (i) δ_1 at Pz, (accounting for 7.9% of the variance), (ii) θ_1 at Pz and CPz (accounting for 7.6% and 4.8% of the variance), and (iii) θ_2 at Cz, CPz, Pz and FCz (accounting for 9.5%, 9.2%, 8.0% and 5.7% of the variance). Discriminant analysis confirmed the independent contribution of these measures at all electrode sites noted.

(iii) Independence of ERP and ERO measures in group discrimination

δ_1 ERO_{EVK} power, δ_1 ERO_{TOT} power, and θ_1 ERO_{TOT} power, all at Pz, and the θ_2 ERO_{TOT} power at Cz were selected as the best⁹ group discriminators. Table 5 shows the results of the MANOVA performed on this set of measures, with an overall significant group effect

($F(4,91) = 4.034, p = 0.005$). The rank order of the discriminant coefficients was the same as for the univariate effect sizes: $ERO_{EVK} \delta_1$ power at Pz, followed by $ERO_{TOT} \theta_2$ power at Cz, $ERO_{TOT} \delta_1$ power at Pz and $ERO_{TOT} \theta_1$ power at Pz.

Table 5 also presents the results of the MANCOVA performed on this subset of ERO measures, with the P3b amplitude at Pz as a covariate. The MANCOVA group effect was not significant ($F(4,90) = 1.833, p = 0.129$) after removal of P3b variance. Although the MANCOVA is non-significant, follow-up univariate analyses are included so that univariate effect sizes can be compared before and after removal of P3b variance. Only θ_2 ERO_{TOT} power at Cz had a p-value below 0.05, providing a weak indication that this measure may provide discriminatory power beyond P3b amplitude.

DISCUSSION

(i) ERP measures

The ERP results concur with those in the alcoholism research literature, with the LTAA group showing a significantly reduced P3b amplitude over central-parietal regions (Begleiter et al., 1984; Begleiter et al., 1987; Benegal et al., 1995; Berman and Noble, 1995; Cohen et al., 1997; Ehlers et al., 2003; Fein and Chang, 2006; Glenn et al., 1994; Glenn et al., 1996; Hill and Steinhauer, 1993; Iacono et al., 2003; Kamarajan et al., 2005; O'Connor et al., 1986; O'Connor et al., 1987; Polich et al., 1994; Porjesz and Begleiter, 1985; 1990; Porjesz et al., 1998; Steinhauer and Hill, 1993; Suresh et al., 2003; Van der Stelt et al., 1998).

Fein and Chang (2006) presented results of between-group ANOVAs of P3b and P3a amplitudes and latencies on this same data. The multi-electrode analysis of the current study confirms the Pz as the primary electrode site for P3b group discrimination, similar to the findings of Rangaswamy et al. (2007). However, the Jones et al (2006) finding of the largest group effect for the P3b amplitude being over the frontal region rather than parietal region, differs from that of both the current study and the literature consensus.

(ii) ERO measures

Our results, as well as the Jones et al. (2006) and Rangaswamy et al. (2007) studies all show that δ ERO_{EVK} power and δ and θ ERO_{TOT} power discriminate the groups¹⁰. There are both similarities and differences across studies in the scalp locations of these findings. We and Rangaswamy et al. (2007) find δ ERO_{EVK} power at parietal sites discriminates the groups, while Jones et al. (2006) reported δ_1 ERO_{EVK} power frontally and the δ_1 ERO_{TOT} power centrally provided the best group discrimination. For θ ERO_{TOT} power, we and Rangaswamy et al.(2007) found best discrimination at central sites, while Jones et al. (2006) found best discrimination frontally. In all three studies, power was reduced in the alcoholic group (LTAAAs or active alcoholics or high-risk of alcoholism) compared to control group for all measures.

The significant group effect on the δ_1 ERO_{EVK} power indicates that the phase-locked (i.e. evoked) activity in the lower δ band discriminates the groups. The δ_1 ERO_{TOT} power, comprising both evoked and non-phase-locked activity also significantly discriminates the groups. As the effect size is smaller for the δ_1 ERO_{TOT} power compared to the δ_1 ERO_{EVK} power, it is most likely that the non-phase-locked activity does not contribute to the significant group effect, and it is only the evoked activity in the lower δ band that account for the significant group differences. Had the non-phase-locked activity contributed, the

⁹As defined in the Methodology section

¹⁰ignoring sub-division of the δ and θ bands, as Rangaswamy et al.(2007) only analyzed these as complete bands

effect size of the δ_1 ERO_{TOT} power would have been larger than the effect size for the δ_1 ERO_{EVK} power. The finding that the θ_1 and θ_2 ERO_{TOT} power measures discriminate the groups, while the θ_1 and θ_2 ERO_{EVK} power measures do not, indicates that it is most likely the contribution of non-phase-locked activity to the θ ERO_{TOT} power that accounts for the significant group effect. If evoked activity discriminated the groups, then the θ ERO_{EVK} power would have shown a significant group effect as well. Only separating the measurement of phase-locked and non-phase-locked power could directly address this issue.

(iii) Independence of the ERO and EPR measures for group discrimination

The group effect sizes for the ERO power and P3b amplitude are of similar magnitude, suggesting that ERO power does not provide more powerful group discrimination than P3b amplitude in this study. After removing P3b amplitude variance, the ERO power measures no longer discriminated the groups, providing strong evidence in this study that ERO power provides an alternative, but not independent measure to P3b amplitude for discriminating LTAAAs from NACs.

Our findings do not support the findings of Jones et al. (2006) and Rangaswamy et al. (2007) that the ERO power measures provide more powerful group discriminators than the ERP amplitude measures. The requisite statistical analyses were not applied to their data to substantiate their conclusions. Our findings cannot be generalized to their data though, as differences in samples (i.e. differences in the population (LTAA vs. active alcoholics vs. individuals at high risk of alcoholism), age and gender of the subjects) and in the experimental paradigm precludes such generalization. From our subject sample, it is not possible to distinguish the effects of predisposition to alcoholism, chronic alcohol abuse and recovery from alcoholism. Further investigation of EROs in populations of active alcoholics and offspring of alcoholics are necessary to address these issues. However, our results do show the importance of appropriate statistical analyses to draw conclusions regarding the relative predictive power of different biomarkers of alcoholism.

In our introduction, two reasons were put forward as to why ERO power measures might provide unique discriminatory information beyond that of ERP amplitude measures. For ERO_{EVK} power measures, it was argued that the temporal extent of the ERO measures across a time interval, rather than at a single time point, could account for the additional discriminatory information. The premise for this argument is that the dynamics or morphology of an ERP component might differ between groups. Our results indicate that this is not the case and any additional information contained in the evoked ERO power measures due to P3b dynamics does not significantly contribute towards group discrimination. The second reason was that in addition to evoked activity, the ERO_{TOT} power measures contains contributions of non-phase-locked activity, and this induced activity might provide additional discriminatory information beyond the ERP amplitude measures. The *post hoc* ERO_{TOT} power finding, although not warranted by the MANCOVA, gives a weak indication that induced θ activity might provide group discriminatory information beyond that of the ERP. This indication of a potential contribution to group discrimination of induced activity should be followed up with a more complete investigation of event-related non-phase-locked activity.

The importance of analyzing event-related phase-locked and non-phase-locked theta activity separately has been highlighted by a number of researchers (Bastiaansen and Hagoort, 2003; Klimesch et al., 1998). A study by Deiber et al. (2007) reported findings on a visual oddball detection task similar to ours, in which evoked and induced oscillatory activity was examined separately. They reported evoked theta activity phase-locked to the visual stimulus and localized to the parieto-occipital region and in parallel, induced theta activity in the form of an ERS over the frontal region. This induced theta activity was found to be

modulated by task load, where increased attentional demand and working memory load resulted in a larger frontal ERS. The evoked parieto-occipital activity did not show modulation to task load. Preliminary analysis on the non-phase-locked activity of our data has revealed a frontally-focused ERS, which is larger in the target compared to non-target stimuli. We are in the process of analyzing these induced oscillations further to investigate their utility as biomarkers for alcoholism and whether they provide independent group discrimination to the ERP amplitude measures.

Acknowledgments

This work was supported by National Institutes for Health, NIH Grants #1R21AA017311, #1R01AA016944 and #2R01AA013659.

References

- American Psychiatric Association. DSM-IV-TR: Diagnostic and Statistical Manual of Mental Disorders. Washington, DC: American Psychiatric Publishing; 2000.
- Basar-Eroglu C, Basar E, Demiralp T, Schurmann M. P300-response: possible psychophysiological correlates in delta and theta frequency channels. A review. *Int J Psychophysiol.* 1992; 13:161–179. [PubMed: 1399755]
- Bastiaansen M, Hagoort P. Event-induced theta responses as a window on the dynamics of memory. *Cortex.* 2003; 39:967–992. [PubMed: 14584562]
- Begleiter H, Porjesz B, Bihari B, Kissin B. Event-related brain potentials in boys at risk for alcoholism. *Science.* 1984; 225:1493–1496. [PubMed: 6474187]
- Begleiter H, Porjesz B, Rawlings R, Eckardt M. Auditory recovery function and P3 in boys at high risk for alcoholism. *Alcohol.* 1987; 4:315–321. [PubMed: 3620101]
- Benegal V, Jain S, Subbukrishna DK, Channabasavanna SM. P300 amplitudes vary inversely with continuum of risk in first degree male relatives of alcoholics. *Psychiatr Genet.* 1995; 5:149–156. [PubMed: 8750356]
- Berman SM, Noble EP. Reduced visuospatial performance in children with the D2 dopamine receptor A1 allele. *Behav Genet.* 1995; 25:45–58. [PubMed: 7755518]
- Berman SM, Whipple SC, Fitch RJ, Noble EP. P3 in young boys as a predictor of adolescent substance use. *Alcohol.* 1993; 10:69–76. [PubMed: 8447968]
- Cohen HL, Porjesz B, Begleiter H, Wang W. Neuroelectric correlates of response production and inhibition in individuals at risk to develop alcoholism. *Biol Psychiatry.* 1997; 42:57–67. [PubMed: 9193742]
- Deiber M-P, Missonnier P, Bertrand O, Gold G, Fazio-Costa L, Ibanez V, Giannakopoulos P. Distinction between Perceptual and Attentional Processing in Working Memory Tasks: A Study of Phase-locked and Induced Oscillatory Brain Dynamics. *Journal of Cognitive Neuroscience.* 2007; 19:158–172. [PubMed: 17214572]
- Delorme A, Makeig S. EEGLAB: an open source toolbox for analysis of single-trial EEG dynamics including independent component analysis. *J Neurosci Methods.* 2004; 134:9–21. [PubMed: 15102499]
- Ehlers CL, Phillips E, Sweeny A, Slawewski CJ. Event-related potential responses to alcohol-related stimuli in African-American young adults: relation to family history of alcoholism and drug usage. *Alcohol Alcohol.* 2003; 38:332–338. [PubMed: 12814900]
- Fein G, Chang M. Visual P300s in long-term abstinent chronic alcoholics. *Alcohol Clin Exp Res.* 2006; 30:2000–2007. [PubMed: 17117965]
- Fell J, Dietl T, Grunwald T, Kurthen M, Klaver P, Trautner P, Schaller C, Elger CE, Fernandez G. Neural bases of cognitive ERPs: more than phase reset. *J Cogn Neurosci.* 2004; 16:1595–1604. [PubMed: 15601521]
- Glenn S, Parsons OA, Sinha R. Assessment of recovery of electrophysiological and neuropsychological functions in chronic alcoholics. *Biol Psychiatry.* 1994; 36:443–452. [PubMed: 7811840]

- Glenn SW, Parsons OA, Smith LT. ERP responses to target and nontarget visual stimuli in alcoholics from VA and community treatment programs. *Alcohol*. 1996; 13:85–92. [PubMed: 8837941]
- Gratton G, Coles MG, Donchin E. A new method for off-line removal of ocular artifact. *Electroenceph clin Neurophysiol*. 1983; 55:468–484. [PubMed: 6187540]
- Gruber WR, Klimesch W, Sauseng P, Doppelmayr M. Alpha phase synchronization predicts P1 and N1 latency and amplitude size. *Cereb Cortex*. 2005; 15:371–377. [PubMed: 15749980]
- Hill SY, Steinhauer SR. Assessment of prepubertal and postpubertal boys and girls at risk for developing alcoholism with P300 from a visual discrimination task. *J Stud Alcohol*. 1993; 54:350–358. [PubMed: 8487544]
- Iacono WG, Malone SM, McGue M. Substance use disorders, externalizing psychopathology, and P300 event-related potential amplitude. *Int J Psychophysiol*. 2003; 48:147–178. [PubMed: 12763572]
- Jones KA, Porjesz B, Chorlian D, Rangaswamy M, Kamarajan C, Padmanabhapillai A, Stimus A, Begleiter H. S-transform time-frequency analysis of P300 reveals deficits in individuals diagnosed with alcoholism. *Clin Neurophysiol*. 2006; 117:2128–2143. [PubMed: 16926113]
- Kamarajan C, Porjesz B, Jones K, Chorlian D, Padmanabhapillai A, Rangaswamy M, Stimus A, Begleiter H. Event-related oscillations in offspring of alcoholics: neurocognitive disinhibition as a risk for alcoholism. *Biol Psychiatry*. 2006; 59:625–634. [PubMed: 16213472]
- Kamarajan C, Porjesz B, Jones KA, Choi K, Chorlian DB, Padmanabhapillai A, Rangaswamy M, Stimus AT, Begleiter H. The role of brain oscillations as functional correlates of cognitive systems: a study of frontal inhibitory control in alcoholism. *Int J Psychophysiol*. 2004; 51:155–180. [PubMed: 14693365]
- Kamarajan C, Porjesz B, Jones KA, Choi K, Chorlian DB, Padmanabhapillai A, Rangaswamy M, Stimus AT, Begleiter H. Alcoholism is a disinhibitory disorder: neurophysiological evidence from a Go/No-Go task. *Biol Psychol*. 2005; 69:353–373. [PubMed: 15925035]
- Klimesch W. EEG alpha and theta oscillations reflect cognitive and memory performance: a review and analysis. *Brain Res Brain Res Rev*. 1999; 29:169–195. [PubMed: 10209231]
- Klimesch W, Russegger H, Doppelmayr M, Pachinger T. A method for the calculation of induced band power: implications for the significance of brain oscillations. *Electroenceph Clin Neurophysiol*. 1998; 108:123–130. [PubMed: 9566625]
- Klimesch W, Schack B, Schabus M, Doppelmayr M, Gruber W, Sauseng P. Phase-locked alpha and theta oscillations generate the P1-N1 complex and are related to memory performance. *Brain Res Cogn Brain Res*. 2004; 19:302–316. [PubMed: 15062867]
- Kolev V, Demiralp T, Yordanova J, Ademoglu A, Isoglu-Alkac U. Time-frequency analysis reveals multiple functional components during oddball P300. *Neuroreport*. 1997; 8:2061–2065. [PubMed: 9223102]
- Makeig S, Westerfield M, Jung TP, Enghoff S, Townsend J, Courchesne E, Sejnowski TJ. Dynamic brain sources of visual evoked responses. *Science*. 2002; 295:690–694. [PubMed: 11809976]
- O'Connor S, Hesselbrock V, Tasman A. Correlates of increased risk for alcoholism in young men. *Prog Neuropsychopharmacol Biol Psychiatry*. 1986; 10:211–218. [PubMed: 3749512]
- O'Connor S, Hesselbrock V, Tasman A, DePalma N. P3 amplitudes in two distinct tasks are decreased in young men with a history of paternal alcoholism. *Alcohol*. 1987; 4:323–330. [PubMed: 3620102]
- Penny WD, Kiebel SJ, Kilner JM, Rugg MD. Event-related brain dynamics. *Trends Neurosci*. 2002; 25:387–389. [PubMed: 12127748]
- Pfurtscheller G, Lopes da Silva FH. Event-related EEG/MEG synchronization and desynchronization: basic principles. *Clin Neurophysiol*. 1999; 110:1842–1857. [PubMed: 10576479]
- Polich J, Pollock VE, Bloom FE. Meta-analysis of P300 amplitude from males at risk for alcoholism. *Psychol Bull*. 1994; 115:55–73. [PubMed: 8310100]
- Porjesz B.; Begleiter, H. Human Brain Electrophysiology and Alcoholism. In: Tarter, R.; Van Thiel, D., editors. *Alcohol and the Brain*. New York: Plenum; 1985. p. 139-182.
- Porjesz B, Begleiter H. Event-related potentials in individuals at risk for alcoholism. *Alcohol*. 1990; 7:465–469. [PubMed: 2222850]

- Porjesz B, Begleiter H. Alcoholism and human electrophysiology. *Alcohol Res Health*. 2003; 27:153–160. [PubMed: 15303626]
- Porjesz B, Begleiter H, Reich T, Van Eerdeghe P, Edenberg HJ, Foroud T, Goate A, Litke A, Chorlian DB, Stimus A, Rice J, Blangero J, Almasy L, Sorbell J, Bauer LO, Kuperman S, O'Connor SJ, Rohrbaugh J. Amplitude of visual P3 event-related potential as a phenotypic marker for a predisposition to alcoholism: preliminary results from the COGA Project. Collaborative Study on the Genetics of Alcoholism. *Alcohol Clin Exp Res*. 1998; 22:1317–1323. [PubMed: 9756048]
- Rangaswamy M, Jones KA, Porjesz B, Chorlian DB, Padmanabhapillai A, Kamarajan C, Kuperman S, Rohrbaugh J, O'Connor SJ, Bauer LO, Schuckit MA, Begleiter H. Delta and theta oscillations as risk markers in adolescent offspring of alcoholics. *Int J Psychophysiol*. 2007; 63:3–15. [PubMed: 17129626]
- Sauseng P, Klimesch W, Gruber WR, Hanslmayr S, Freunberger R, Doppelmayr M. Are Event-Related Potential Components Generated By Phase Resetting Of Brain Oscillations? A Critical Discussion. *Neuroscience*. 2007; 146:1435–1444. [PubMed: 17459593]
- Schurmann M, Basar-Eroglu C, Kolev V, Basar E. Delta responses and cognitive processing: single-trial evaluations of human visual P300. *Int J Psychophysiol*. 2001; 39:229–239. [PubMed: 11163900]
- Shah AS, Bressler SL, Knuth KH, Ding M, Mehta AD, Ulbert I, Schroeder CE. Neural dynamics and the fundamental mechanisms of event-related brain potentials. *Cereb Cortex*. 2004; 14:476–483. [PubMed: 15054063]
- Steinhauer SR, Hill SY. Auditory event-related potentials in children at high risk for alcoholism. *J Stud Alcohol*. 1993; 54:408–421. [PubMed: 8341043]
- Suresh S, Porjesz B, Chorlian DB, Choi K, Jones KA, Wang K, Stimus A, Begleiter H. Auditory P3 in female alcoholics. *Alcohol Clin Exp Res*. 2003; 27:1064–1074. [PubMed: 12878912]
- Van der Stelt O, Geesken R, Gunning WB, Snel J, Kok A. P3 scalp topography to target and novel visual stimuli in children of alcoholics. *Alcohol*. 1998; 15:119–136. [PubMed: 9476958]
- Yordanova J, Rosso OA, Kolev V. A transient dominance of theta event-related brain potential component characterizes stimulus processing in an auditory oddball task. *Clin Neurophysiol*. 2003; 114:529–540. [PubMed: 12705433]

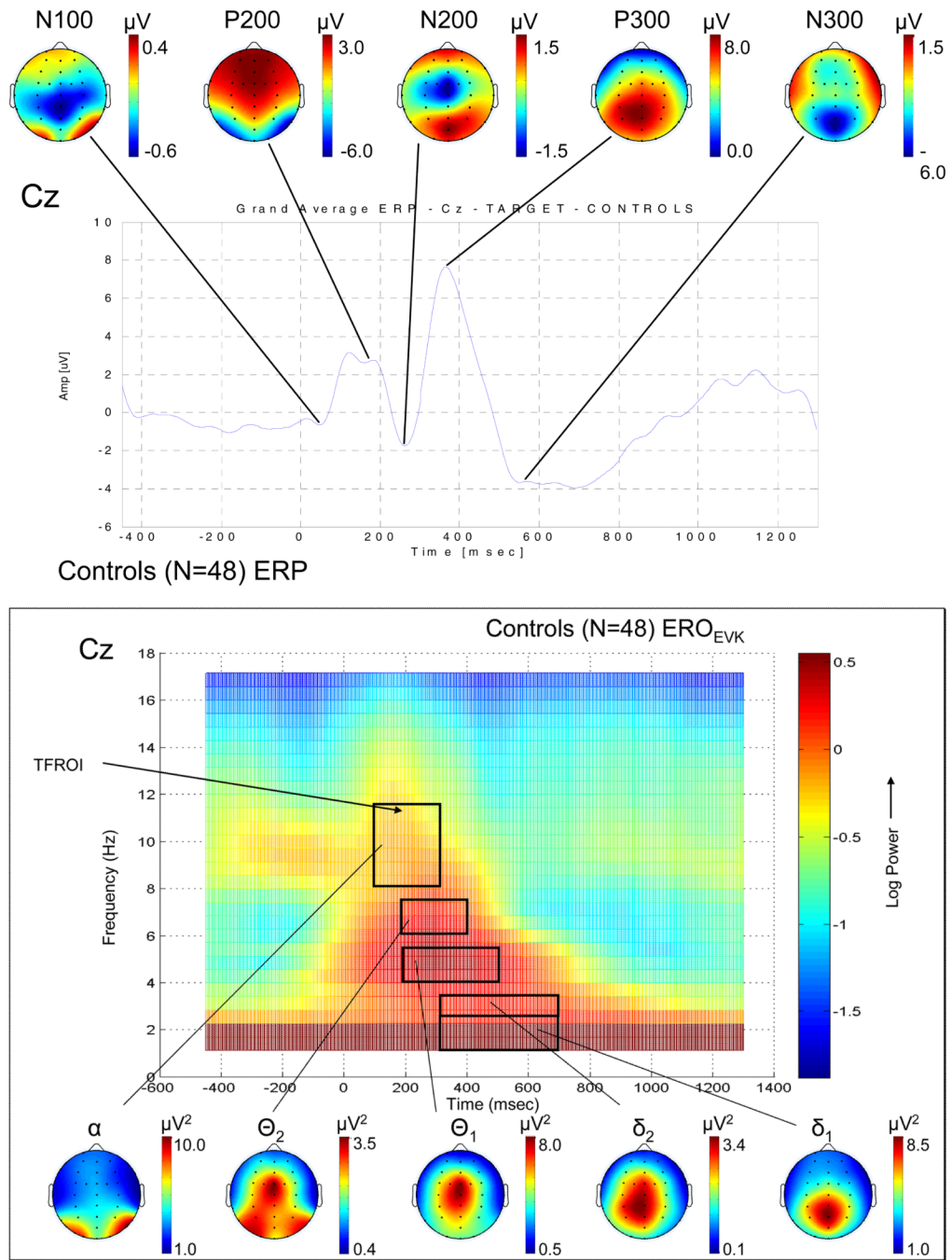


Figure 1. Comparison of ERP and ERO measures derived from the event-related data for the target condition for the NACs. (a) The grand average ERP waveform for electrode site Cz is displayed, along with the grand average topographical maps for each of the major ERP components, namely the N100, P200, N200, P300 (P3b) and N300. (b) The grand average ERO_{EVK} TFR for the Cz electrode site is shown, together with the grand average topographical maps for the TFROIs given in Table 2.

Table 1

MANOVA results for the between-group analyses of each of the major ERP amplitude components (N100, P200, N200, P300 (P3b) and N300), with the multiple dependent variables taken as the particular ERP amplitude measure at the midline electrodes Fz, FCz, Cz, CPz and Pz. Follow-up univariate ANOVAs with each of the dependent variables taken independently and follow-up discriminant analysis with the dependent variables taken as the predictors in the discriminant function are shown for MANOVAs where the group effect is significant at $p \leq 0.05$.

ERP Amplitude Measures		Model: Fz, FCz, Cz, PCz, Pz		
N100 amplitude				
MANOVA Group (N=67; 37 NACs, 30 LTAAAs) Error df = 61	df		Pillai-Bartlett Trace	F-value
	5		.103	1.408
P200 amplitude				
MANOVA Group (N = 85; 42 NACs; 43 LTAAAs) Error df = 79	df		Pillai-Bartlett Trace	F-value
	5		.139	2.546*
<i>MANOVA Follow-up Analyses</i>				
Univariate ANOVAs				
	df	Controls Mean Amplitude	LTAAs Mean Amplitude	Effect Size (% Variance) Group
Dependant Variables				
P200 amplitude at Fz	1	5.77	5.92	0.1
P200 amplitude at FCz	1	6.14	6.30	0.1
P200 amplitude at Cz	1	6.29	5.92	0.3
P200 amplitude at CPz	1	6.70	6.25	0.4
P200 amplitude at Pz	1	7.12	6.30	1.5
Discriminant Analysis				
			Wilks' Lambda	% Classification Accuracy
			0.861*	64.7
Predictors				
		Standardized Canonical Discriminant Function Coefficients		
P200 amplitude at Fz			2.00	
P200 amplitude at FCz			-5.16	
P200 amplitude at Cz			5.71	
P200 amplitude at CPz			-4.63	
P200 amplitude at Pz			2.60	
N200 amplitude				
MANOVA Group (N=88; 44 NACs, 44 LTAAAs) Error df = 82	df		Pillai-Bartlett Trace	F-value
	5		.116	2.162
P300 (P3b) amplitude				
MANOVA Group (N = 96; 48 NACs; 48 LTAAAs) Error df = 90	df		Pillai-Bartlett Trace	F-value

ERP Amplitude Measures		Model: Fz, FCz, Cz, PCz, Pz		
	5		.195	4.353**
<i>MANOVA Follow-up Analyses</i>				
Univariate ANOVAs				
	df	Controls Mean Amplitude	LTAAs Mean Amplitude	Effect Size (% Variance) Group
Dependant Variables				
P300 amplitude at Fz	1	7.99	8.02	0.0
P300 amplitude at FCz	1	10.40	9.06	1.8
P300 amplitude at Cz	1	11.85	9.94	3.2
P300 amplitude at CPz	1	12.97	10.65	4.8*
P300 amplitude at Pz	1	12.80	9.93	8.5**
Discriminant Analysis			Wilks' Lambda	% Classification Accuracy
			0.805***	68.8
Predictors		Standardized Canonical Discriminant Function Coefficients		
P300 amplitude at Fz			-1.89	
P300 amplitude at FCz			2.13	
P300 amplitude at Cz			1.13	
P300 amplitude at CPz			-3.74	
P300 amplitude at Pz			2.72	
N300 amplitude				
MANOVA	df		Pillai-Bartlett Trace	F-value
Group (N = 96; 48 NACs; 48 LTAAs)				
Error df = 90				
	5		.097	1.924

Effect is significant:

* $p \leq 0.05$;

** $p \leq 0.01$;

*** $p \leq 0.001$.

Table 2

Time-frequency region of interest (TFROI) used for the evoked and total ERO power analysis.

ERO bands	Lower frequency [Hz]	Upper frequency [Hz]	Min. Time [ms]	Max. Time [ms]
δ_1 (1–2 Hz)	1.14	2.28	300	700
δ_2 (3–3 Hz)	2.85	3.42	300	700
Θ_1 (4–5 Hz)	4.00	5.71	200	500
Θ_2 (6–7 Hz)	6.28	7.42	200	400
α (8–12 Hz)	8.00	11.42	100	300

Table 3

MANOVA results for the between-group analyses of each of the ERO_{EVK} power measures (δ_1 , δ_2 , θ_1 , θ_2 and α) with the multiple dependent variables taken as the particular log-transformed ERO_{EVK} power measure at the midline electrodes Fz, FCz, Cz, CPz and Pz. Follow-up univariate ANOVAs with each of the dependent variables taken independently and follow-up discriminant analysis with the dependent variables taken as the predictors in the discriminant function are shown for MANOVAs where the group effect is significant at $p < 0.05$.

Model: log(Fz), log(FCz), log(Cz), log(PCz), log(Pz) Group (N = 96; 48 NACs, 48 LTAs) MANOVA: Error df = 90			
Evoked ERO Power Measures			
ERO_{EVK} power			
δ_1 (1–2 Hz, 300–700ms)			
MANOVA	df	Pillai-Bartlett Trace	F-value
	5	.147	3.098*
<i>MANOVA Follow-up Analyses</i>			
Univariate ANOVAs			
Dependant Variables showing significance	df	Controls Mean Log Power	LTAAs Mean Log Power
δ_1 ERO_{EVK} power at Fz		0.380	0.372
δ_1 ERO_{EVK} power at FCz		0.522	0.387
δ_1 ERO_{EVK} power at Cz	1	0.640	0.443
δ_1 ERO_{EVK} power at CPz	1	0.758	0.539
δ_1 ERO_{EVK} power at Pz	1	0.808	0.533
Discriminant Analysis		Wilks' Lambda	% Classification Accuracy
		0.853*	64.6
Predictors		Standardized Canonical Discriminant Function Coefficients	
δ_1 ERO_{EVK} power at Fz		-1.04	
δ_1 ERO_{EVK} power at FCz		1.27	
δ_1 ERO_{EVK} power at Cz		-0.21	
δ_1 ERO_{EVK} power at CPz		-0.99	
δ_1 ERO_{EVK} power at Pz		1.55	
<hr/>			
ERO_{EVK} power			
δ_2 (3–3 Hz, 300–700ms)			
MANOVA	df	Pillai-Bartlett Trace	F-value
	5	.094	1.858
<hr/>			
ERO_{EVK} power			
θ_1 (4–5 Hz, 200–500ms)			
MANOVA	df	Pillai-Bartlett Trace	F-value
	5	.082	1.608
<hr/>			
ERO_{EVK} power			
θ_2 (6–7 Hz, 200–400ms)			

Evoked ERO Power Measures		Model: log(Fz), log(FCz), log(Cz), log(PCz), log(Pz) Group (N = 96; 48 NACs, 48 LTAs) MANOVA: Error df =90	
MANOVA	df	Pillai-Bartlett Trace	F-value
	5	.086	1.699
<hr/>			
ERO _{EVK} power α (8–12 Hz, 100–300ms)			
MANOVA	df	Pillai-Bartlett Trace	F-value
	5	.064	1.221

Effect is significant:

* $p \leq 0.05$;

** $p \leq 0.01$;

*** $p \leq 0.001$.

Table 4

MANOVA results for the between-group analyses of each of the ERO_{TOT} power measures (δ_1 , δ_2 , θ_1 , θ_2 and α) with the multiple dependent variables taken as the particular log-transformed ERO_{TOT} power measure at the midline electrodes Fz, FCz, Cz, CPz and Pz. Follow-up univariate ANOVAs with each of the dependent variables taken independently and follow-up discriminant analysis with the dependent variables taken as the predictors in the discriminant function are shown for MANOVAs where the group effect is significant at $p < 0.05$.

Model: $\log(Fz)$, $\log(FCz)$, $\log(Cz)$, $\log(PCz)$, $\log(Pz)$ Group (N = 96; 48 NACs, 48 LTAAAs) MANOVA: Error df = 90				
Total ERO Power Measures				
ERO_{TOT} power				
δ_1 (1–2 Hz, 300–700ms)				
MANOVA	df		Pillai-Bartlett Trace	F-value
	5		.161	3.452**
<i>MANOVA Follow-up Analyses</i>				
Univariate ANOVAs				
	df	Controls Mean Log Power	LTAAs Mean Log Power	Effect Size (% Variance) Group
Dependant Variables				
δ_1 ERO _{TOT} power at Fz	1	1.031	1.048	0.3
δ_1 ERO _{TOT} power at FCz	1	1.106	1.084	0.4
δ_1 ERO _{TOT} power at Cz	1	1.157	1.110	1.4
δ_1 ERO _{TOT} power at CPz	1	1.209	1.129	3.4
δ_1 ERO_{TOT} power at Pz	1	1.228	1.102	7.9**
Discriminant Analysis			Wilks' Lambda	% Classification Accuracy
			0.839**	68.8
Predictors				
Standardized Canonical Discriminant Function Coefficients				
δ_1 ERO _{TOT} power at Fz			-1.32	
δ_1 ERO_{TOT} power at FCz			1.93	
δ_1 ERO_{TOT} power at Cz			-1.77	
δ_1 ERO _{TOT} power at CPz			-0.19	
δ_1 ERO_{TOT} power at Pz			1.70	
<hr/>				
ERO _{TOT} power				
δ_2 (3-3 Hz, 300–700ms)				
MANOVA	df		Pillai-Bartlett Trace	F-value
	5		.089	1.766
<hr/>				
ERO_{TOT} power				
Θ_1 (4–5 Hz, 200–500ms)				
MANOVA	df		Pillai-Bartlett Trace	F-value
	5		.125	2.567*
<i>MANOVA Follow-up Analyses</i>				
Univariate ANOVAs				

Model: log(Fz), log(FCz), log(Cz), log(PCz), log(Pz)				
Group (N = 96; 48 NACs, 48 LTAAAs)				
MANOVA: Error df =90				
Total ERO Power Measures				
	df	Controls Mean Log Power	LTAAAs Mean Log Power	Effect Size (% Variance) Group
Dependant Variables				
Θ_1 ERO _{TOT} power at Fz		1.260	1.272	0.1
Θ_1 ERO _{TOT} power at FCz		1.373	1.349	0.3
Θ_1 ERO _{TOT} power at Cz		1.363	1.301	2.0
Θ_1 ERO _{TOT} power at CPz	1	1.322	1.227	4.8*
Θ_1 ERO _{TOT} power at Pz	1	1.254	1.133	7.6**
Discriminant Analysis			Wilks' Lambda	% Classification Accuracy
			0.875*	68.8
Predictors		Standardized Canonical Discriminant Function Coefficients		
Θ_1 ERO _{TOT} power at Fz			-0.76	
Θ_1 ERO _{TOT} power at FCz			0.16	
Θ_1 ERO _{TOT} power at Cz			-0.06	
Θ_1 ERO _{TOT} power at CPz			-0.57	
Θ_1 ERO _{TOT} power at Pz			1.69	
ERO_{TOT} power				
Θ_2 (6-7 Hz, 200-400ms)				
MANOVA	df		Pillai-Bartlett Trace	F-value
	5		.120	2.461*
<i>MANOVA Follow-up Analyses</i>				
Univariate ANOVAs				
	df	Controls Mean Log Power	LTAAAs Mean Log Power	Effect Size (% Variance) Group
Dependant Variables				
Θ_2 ERO _{TOT} power at Fz		1.122	1.042	2.7
Θ_2 ERO _{TOT} power at FCz	1	1.205	1.093	5.7*
Θ_2 ERO _{TOT} power at Cz	1	1.185	1.034	9.5**
Θ_2 ERO _{TOT} power at CPz	1	1.133	0.978	9.2**
Θ_2 ERO _{TOT} power at Pz	1	1.070	0.927	8.0**
Discriminant Analysis			Wilks' Lambda	% Classification Accuracy
			.880*	61.5
Predictors		Standardized Canonical Discriminant Function Coefficients		
Θ_2 ERO _{TOT} power at Fz		-0.90		
Θ_2 ERO _{TOT} power at FCz		-0.07		
Θ_2 ERO _{TOT} power at Cz		2.29		
Θ_2 ERO _{TOT} power at CPz		-0.95		
Θ_2 ERO _{TOT} power at Pz		0.33		
ERO _{TOT} power				

Model: log(Fz), log(FCz), log(Cz), log(PCz), log(Pz) Group (N = 96; 48 NACs, 48 LTAAAs) MANOVA: Error df =90			
Total ERO Power Measures			
$\alpha(8-12 \text{ Hz}, 100-300\text{ms})$			
MANOVA	df	Pillai-Bartlett Trace	F-value
	5	.078	1.532

Effect is significant:

* $p \leq 0.05$;

** $p \leq 0.01$;

*** $p \leq 0.001$.

Table 5

MANOVA and MANCOVA results for the between-group analyses of a compact model comprising the log-transformed δ_1 ERO_{EVK} power at electrode site Pz, the log-transformed δ_1 ERO_{TOT} power at electrode site Pz, the log-transformed θ_1 ERO_{TOT} power at electrode site Pz and the log-transformed θ_2 ERO_{TOT} power at electrode site Cz. Follow-up univariate ANOVAs (ANCOVAs) with each of the dependent variables taken independently and follow-up discriminant analysis with the dependent variables taken as the predictors in the discriminant function (for the MANOVAs only) are also shown for the MANOVAs (MANCOVAs).

Selected ERO Power Measures in Compact Model					Model: $\log(\text{Pz-}\delta_1\text{-ERO}_{\text{EVK}})$, $\log(\text{Pz-}\delta_1\text{-ERO}_{\text{TOT}})$, $\log(\text{Pz-}\Theta_1\text{-ERO}_{\text{TOT}})$, $\log(\text{Cz-}\Theta_2\text{-ERO}_{\text{TOT}})$	
					Group (N = 96)	
					MANOVA: Error df = 91	
δ_1 ERO_{EVK} power (1–2 Hz, 300–700ms) at Pz and δ_1 ERO_{TOT} power (1–2 Hz, 300–700ms) at Pz and Θ_1 ERO_{TOT} power (4–5 Hz, 200–500ms) at Pz and Θ_2 ERO_{TOT} power (6–7 Hz, 200–400ms) at Cz						
MANOVA	df		Pillai-Bartlett Trace		F-value	
<i>MANOVA Follow-up Analyses</i>	4		.151		4.034**	
Univariate ANOVAs						
Dependant Variables	df	Controls Mean Log Power	LTAAs Mean Log Power		Effect Size (% Variance) Group	
δ_1 ERO_{EVK} at Pz	1	0.808	0.533		9.9**	
δ_1 ERO_{TOT} at Pz	1	1.228	1.102		7.9**	
Θ_1 ERO_{TOT} at Pz	1	1.254	1.133		7.6**	
Θ_2 ERO_{TOT} at Cz	1	1.185	1.034		9.5**	
Discriminant Analysis						
			Wilks' Lambda		% Classification Accuracy	
			0.849**		68.8	
Predictors						
			Standardized Canonical Discriminant Function Coefficients			
δ_1 ERO _{EVK} at Pz			0.939			
δ_1 ERO _{TOT} at Pz			-0.440			
Θ_1 ERO _{TOT} at Pz			0.264			
Θ_2 ERO _{TOT} at Cz			0.504			
MANCOVA						
Covariate – ERP P300 (P3b) Amplitude			Pillai-Bartlett Trace		F-value	
			.075		1.833	
<i>MANCOVA Follow-up Analyses</i>						
Univariate ANCOVAs						
Dependant Variables	df	Controls Marginal Mean Log Power	LTAAs Marginal Mean Log Power		Effect Size (% Variance) Group	
δ_1 ERO _{EVK} at Pz	1	0.700	0.642		1.6	
δ_1 ERO _{TOT} at Pz	1	1.177	1.153		0.7	
Θ_1 ERO _{TOT} at Pz	1	1.221	1.166		2.1	
Θ_2 ERO_{TOT} at Cz	1	1.156	1.062		4.3*	

Effect is significant:

* $p \leq 0.05$;

**
 $p \leq 0.01$;

 $p \leq 0.001$.